

Analysis of the Reactive Element Effect on the Oxidation of Ceria Doped Nickel

R. W. Jackson · J. P. Leonard · L. Niewolak ·
W. J. Quadakkers · R. Murray · S. Romani ·
G. J. Tatlock · F. S. Pettit · G. H. Meier

Received: 7 March 2012 / Published online: 22 May 2012
© Springer Science+Business Media, LLC 2012

Abstract The effects of external doping with CeO₂ on the oxidation of nickel have been evaluated. The materials studied were pure Ni and Ni with the surface doped with CeO₂ by pulsed laser deposition. The oxidation kinetics were measured using thermogravimetric analysis. The oxidation microstructures were observed by scanning electron microscopy and cross-sectional transmission electron microscopy. Compositional analysis was performed with energy dispersive X-ray analysis and sputtering neutrals mass spectrometry. Phase identification was performed using X-ray diffraction. Doping with CeO₂ resulted in a significant decrease in the NiO growth rate at intermediate temperatures, e.g. 800 °C. The scales on doped Ni grew primarily inward whereas those on the undoped Ni grew primarily outward. Deposition of the CeO₂ dopant onto Ni with a thin, preformed NiO layer produced a similar reduction in the subsequent NiO growth rate. The CeO₂ dopant did not reduce the growth rate at high temperature (1,300 °C). The results indicate that the CeO₂ dopant influences grain boundary transport in the NiO. Mechanisms are presented to attempt to describe the above observations.

Keywords Nickel oxide · Reactive element effect · Oxidation kinetics

R. W. Jackson · J. P. Leonard · F. S. Pettit · G. H. Meier (✉)
Department of Mechanical Engineering and Materials Science, University of Pittsburgh, Pittsburgh,
PA, USA
e-mail: ghmeier@pitt.edu

L. Niewolak · W. J. Quadakkers
Forschungszentrum Jülich, IEF-2, 52428 Jülich, Germany

R. Murray · S. Romani · G. J. Tatlock
Centre for Materials and Structures, School of Engineering, University of Liverpool, Liverpool, UK

Introduction

In previous work, nickel and nickel alloys were investigated as possible interconnect materials for use in solid oxide fuel cells [1, 2]. Pure nickel coated with CeO_2 was found to oxidize very slowly compared to undoped Ni. These results were interpreted in terms of the reactive element effect (REE).

The addition of small concentrations of reactive elements (RE) such as Y, Zr, La, and Ce have been found to improve the oxidation resistance of many alloys and decrease the growth rate of NiO [1–6]. The mechanism by which the reactive element can slow transport in the oxide scale, is not fully agreed upon, and may differ for different oxide/RE systems. Two popularly supported mechanisms are the grain boundary blocking mechanism in which the RE segregates to oxide grain boundaries [7–9], inhibiting grain boundary diffusion, and the poisoned interface model (PIM), in which the RE segregate to the oxide/metal interface, retarding the interface reaction [10–13]. In this investigation, the effect of the reactive element is studied when it is allowed to contact the metal-alloy interface, and when it is deliberately separated from this interface.

Experimental Procedures

High purity nickel (Goodfellow Ltd. 99.999 %) was oxidized with and without a CeO_2 dopant layer on the surface. The specimens were ground to a 600 grit finish using SiC papers, and were ultrasonically cleaned in water, acetone, and isopropanol. Pulsed laser deposition (PLD) was used to deposit a 100–200 nm thick ceria coating onto nickel. The experimental procedure was previously described [1].

Thermogravimetric analysis (TGA) was performed at 800 °C using a Cahn C1000 microbalance in dry air, in a vertical furnace. Additional air exposures were performed at 800 and 1,300 °C in a separate furnace.

Plasma sputtered neutral mass spectrometry (SNMS) was performed using an INA-3 spectrometer (Specs GmbH), using Ar-plasma as a medium in the high frequency (HFM) sputtering mode [14]. The collected data were quantified using the procedure described in Ref. [15]. The sputtered surface in each measurement had a diameter of 3 mm.

Cross-section specimens for transmission electron microscopy (TEM) were prepared using a focused ion beam (FIB) technique. A JEOL 2000FX TEM operated at 200 kV was used to record images and diffraction patterns from the FIB cross-sections. EDS analysis of the levels of segregation to the oxide grain boundaries was then carried out in a VG HB601 STEM at an operating voltage of 100 kV.

Results

The oxidation behavior of nickel at 800 °C was found to be drastically changed by the deposition of a thin film of CeO_2 onto the surface of the specimen. This is

demonstrated in the morphology of the oxide scale, shown in Fig. 1. NiO grown on nickel is fibrous while the NiO formed on CeO₂ coated nickel is in the form of mounds that are approximately 2 μm high. The difference between the two oxide scales is also prominent when the scales are viewed in cross section. The thickness of the scale on the uncoated Ni is greater than that on the coated specimen by roughly a factor of four. The scale on the coated Ni shows a greater thickness variation as expected from the surface micrographs.

Following oxidation, there is no distinct CeO₂ layer found across the surface of the exposed specimen. There are ceria particles that can be found at the outside of the scale as seen in Fig. 1d. The presence of these particles near the gas/oxide interface suggests that the scale is growing primarily inward whereas undoped NiO grows primarily outward. The change in growth direction is a common result of the REE.

The concentration profiles across the scales were further analyzed by SNMS. The profiles for the specimen with the CeO₂ deposited directly onto the Ni (Fig. 2) show that Ce is mostly concentrated close to scale/gas interface, however, still covered by a thin NiO layer with substantially lower Ce concentration.

Figure 3 presents dark field and bright field images of the scale formed on a CeO₂-doped specimen which was oxidized at 800 °C for fifty hours. Figure 4 presents EDS spectra corresponding to six locations in the scale. The columnar grains below the ceria rich layer are nickel oxide containing small particles of cerium rich oxide. The grain boundaries between these columnar grains contain cerium, with none detected in the grains themselves. However the amount of cerium on the boundaries varies from boundary to boundary (see spectra 1, 2 and 3). All the grain boundary spectra were collected from a 10 × 10 nm box sitting astride the

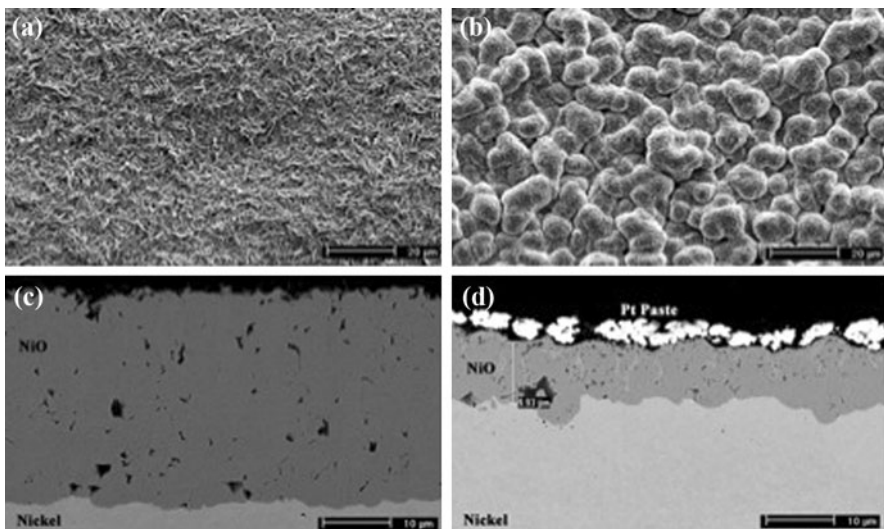


Fig. 1 Surface micrographs of **a** uncoated and **b** CeO₂ coated Ni exposed in air for 500 h at 800 °C. **c** and **d** are the corresponding cross-sectional micrographs

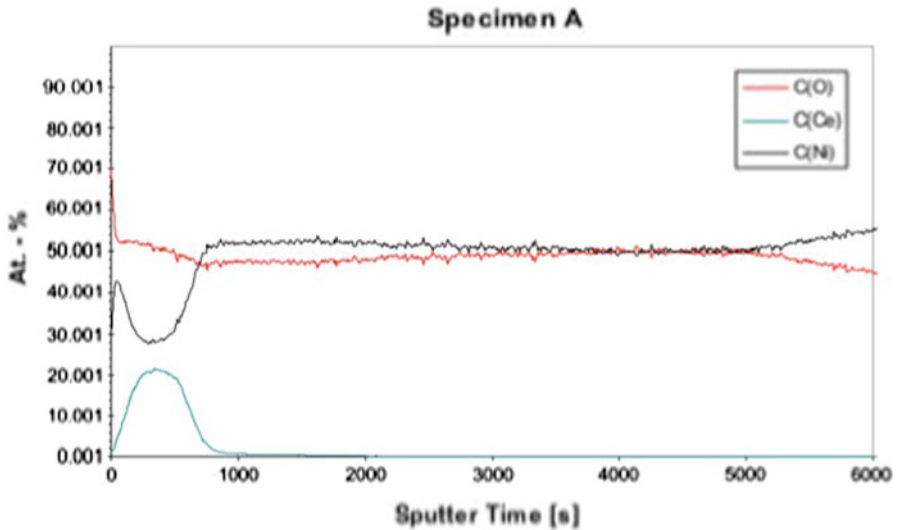


Fig. 2 SNMS depth profile in the outer part of the NiO scale formed on Ni with a CeO₂ dopant layer. The sputter time of 5,500 s approximately corresponds to the oxide/metal interface

grain boundary. Deeper into the nickel oxide, the amount of cerium on the grain boundaries decreases quickly to nearly the minimum level of detection (see spectrum 4). Quantification for this spectrum suggests a maximum Ce level of 0.3 at.% in the volume sampled. There is no detectable Ce at the metal/oxide interface, with the possible exception of some of the triple points where the oxide grain boundaries meet the metal/oxide interface. Here the Ce level is also at the limit of detection (spectrum 5). In the nickel oxide above the ceria rich layer (near the oxide-gas interface), there is also ceria on the grain boundaries. Indeed, probably rather more than in the grain boundaries below the ceria rich layer (spectrum 6).

Figures 5 and 6 show the effects of CeO₂ doping on the oxidation of Ni at 1,300 °C. The surface of the undoped surface (Fig. 5a) indicates a larger NiO grain size than that for the doped surface (Fig. 5b.). However, the scale thicknesses are identical for the two specimens indicating the REE is not significant at this temperature.

These results clearly demonstrate that reactive element additions can substantially decrease the growth rate of NiO at 800 °C. However, the mechanism that produces this change is unclear. As described in the introduction, one proposal is the PIM. In an attempt to investigate the feasibility of the PIM, two nickel sheets were pre-oxidized for 15 min at 800 °C producing an approximately 1 μm thick scale. One of the oxidized coupons was coated with CeO₂ and then both coupons were exposed for an additional 50 h. The oxidation kinetics of two preoxidized Ni specimens were measured by TGA at 800 °C. The results (Fig. 7) indicate that the rate reduction caused by CeO₂ occurs from the earliest exposure time recorded.

Following this exposure, the surface of pre-oxidized and CeO₂ coated specimens appeared similar to the surfaces of the coated nickel that had not received the

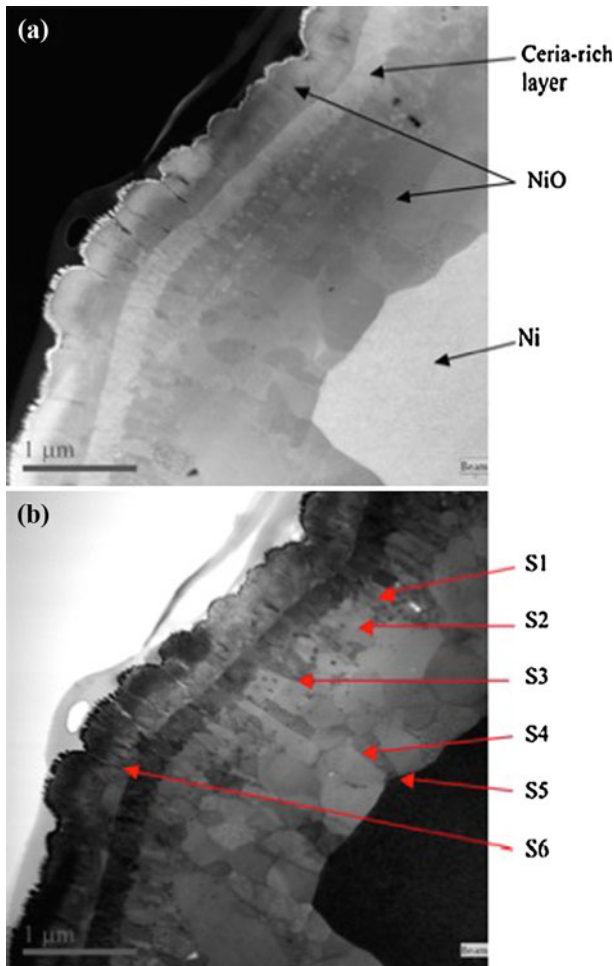
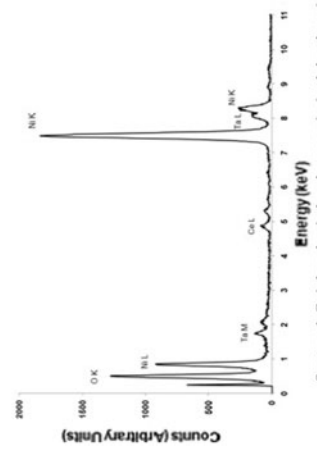


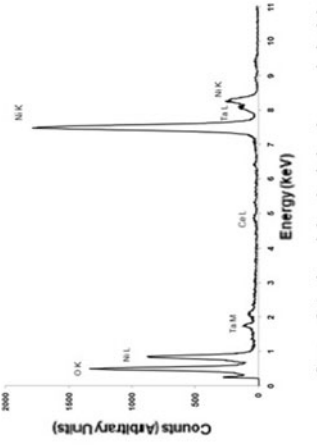
Fig. 3 **a** Dark field and **b** bright field images of the scale formed on a CeO_2 -doped specimen which was oxidized at 800°C for 50 h. S1-S6 refer to the typical positions from which the spectra shown in Fig. 4 were acquired

pre-oxidation treatment. Cross sectional micrographs (Fig. 8) show that the scale thickness is reduced for the coated nickel with respect to the uncoated nickel. The pre-oxidized and coated nickel has a thicker scale than the non-pre-oxidized coated nickel (Fig. 1d), but this difference is attributed to the initial oxide growth that occurred prior to coating.

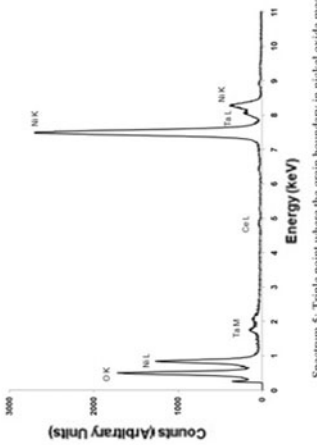
Figure 9 presents the SNMS profiles for the specimen which was oxidized for 15 min at 800°C in air, coated with CeO_2 following pre-oxidation and then re-exposed for 50 h. These results are qualitatively similar to those achieved on the Ni-substrate coated with ceria before oxidation (Fig. 2). However, the overall Ce concentration is substantially smaller than that measured in the sample coated with ceria before oxidation. These results are more easily quantifiable than those in Fig. 2



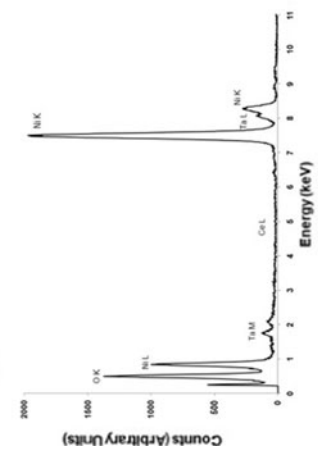
Spectrum 1: Grain boundary in the columnar grains just below the ceria layer.



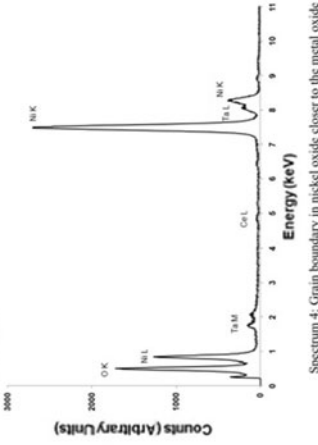
Spectrum 3: Another grain boundary in the columnar grains just below the ceria layer.



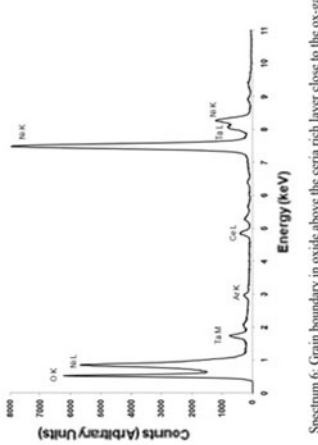
Spectrum 5: Triple point where the grain boundary in nickel oxide meets the metal oxide interface.



Spectrum 2: Grain center in the columnar grains just below the ceria layer.



Spectrum 4: Grain boundary in nickel oxide closer to the metal oxide interface.



Spectrum 6: Grain boundary in oxide above the ceria rich layer close to the ox-gas interface.

- ◀ **Fig. 4** EDs spectra from six locations in the scale from Fig. 3. *Spectrum 1* grain boundary in the columnar grains just below the ceria layer. *Spectrum 2* grain center in the columnar grains just below the ceria layer. *Spectrum 3* another grain boundary in the columnar grains just below the ceria layer. *Spectrum 4* grain boundary in nickel oxide closer to the metal-oxide interface. *Spectrum 5* triple point where the grain boundary in nickel oxide meets the metal-oxide interface. *Spectrum 6* grain boundary in nickel oxide above the ceria rich layer closer to the oxide-gas interface

since the scale/gas interface remains relatively planar. The profiles show that Ce is concentrated in the outer regions, but not immediately at the gas-oxide interface. The Ce signal has dropped to the background level in the inner part of the scale and at the scale/metal interface.

Figure 10 presents TEM images of the specimen which was oxidized for 15 min at 800 °C in air, coated with CeO₂ following pre-oxidation and then re-exposed for 50 h. The pre-oxidation treatment created a dense, continuous barrier between the metal-oxide interface and the surface of the oxide. This barrier did not allow the deposited ceria to contact unoxidized nickel and the reduction of the growth rate of NiO was still observed. The only possibility of the ceria affecting the metal-oxide interface would occur if cerium could be transported through 1 μm of NiO during exposure. EDS and SNMS measurements only indicated ceria in the outer portion of the scale.

Discussion

The key results described above are:

- Surface doping with CeO₂ greatly decreases the oxidation rate of Ni at 800 °C and changes the scale growth direction from primarily outward to inward.

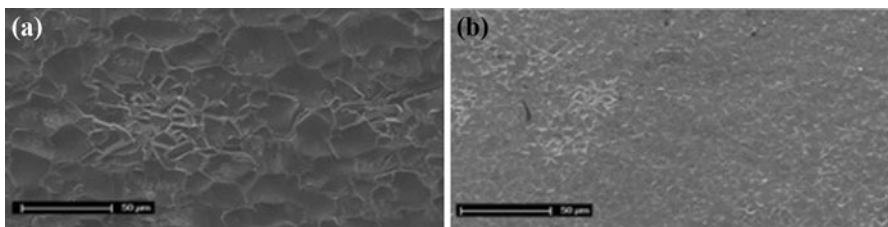


Fig. 5 Surfaces of pure Ni oxidized for 1 h at 1,300 °C. **a** undoped Ni, **b** CeO₂-doped Ni

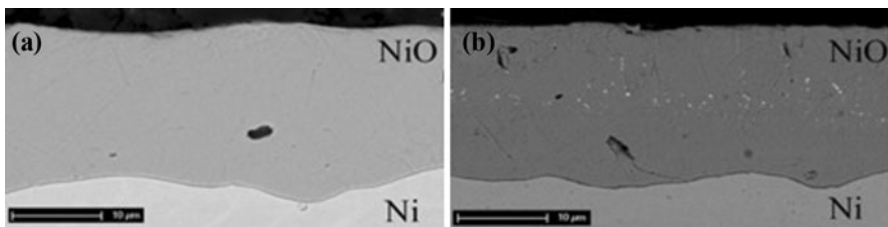


Fig. 6 Cross-sections of pure Ni oxidized for 1 h at 1,300 °C. **a** undoped Ni, **b** CeO₂-doped Ni

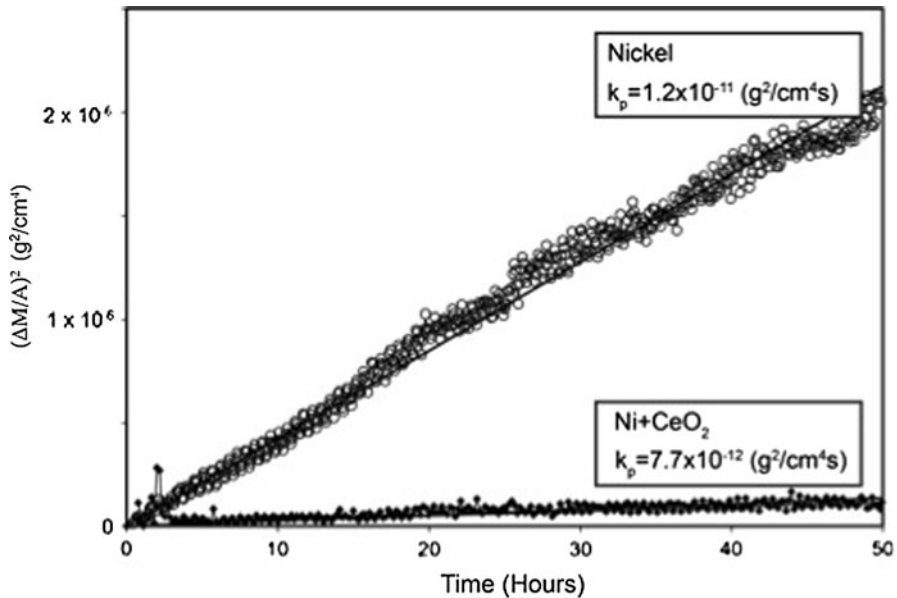


Fig. 7 Weight change versus square root of time at 800 °C for two preoxidized Ni specimens, one with and one without a CeO₂ dopant layer applied to the preformed NiO layer

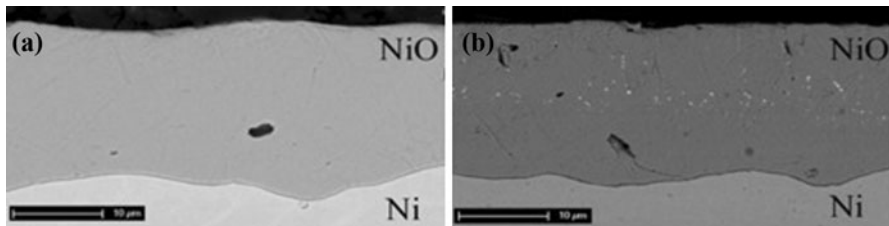


Fig. 8 Cross-sections of nickel which was oxidized for 15 min at 800 °C in air and then **a** re-exposed for 50 h, and **b** a separate specimen which was coated with CeO₂ following pre-oxidation and then re-exposed for 50 h

- The surface doping has negligible effect on the growth rate at 1,300 °C.
- The CeO₂ also decreases the scale growth rate on preoxidized Ni at 800 °C from the beginning of the exposure.
- There is no indication by either EDS or SNMS that Ce ions reached the Ni/NiO interface during exposure of the preoxidized Ni.
- XTEM analysis showed that a continuous layer of Ce rich oxide was present after 50 h oxidation at 800 °C across much of the sample.

The mechanism associated with these observations is of major interest. Haugrud [6] has summarized numerous observations for the oxidation of Ni which had been coated with thin layers of CeO₂, La₂O₃ and SiO₂. All three surface dopants reduced the growth rate of the NiO scale. The results for CeO₂ were comparable to those

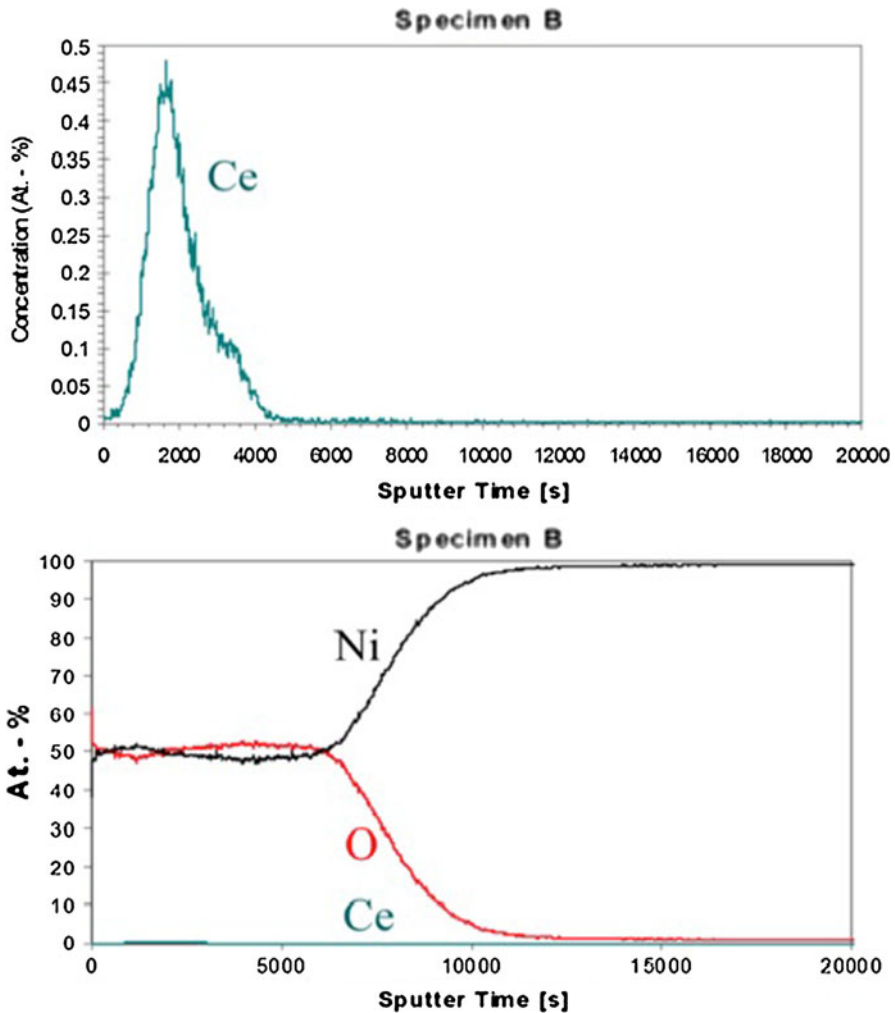


Fig. 9 SNMS depth profile of NiO scale formed on Ni with a CeO₂ dopant layer deposited on a preformed NiO layer. *Lower figure* showing overview of Ni, O, Ce concentration, *upper figure* illustrating differently magnified vertical axis to illustrate Ce distribution

from the present study in that the dopant slowed the oxidation rate at 800 °C but became less effective at high temperatures, e.g. 1,200 °C. The p_{O_2} -dependence of the parabolic rate constants for NiO growth was the same for doped and undoped ($\propto p_{O_2}^{1/6}$) specimens which is typically considered to indicate scale growth dominated by Ni cation diffusion over cation vacancies (V''_{Ni}). Cross-section TEM investigation of the La₂O₃-doped Ni indicated the La₂O₃ particles were in the outer portion of the scale indicating a change in growth direction. The CeO₂-doped specimens were not examined by TEM. Haugsrud concludes that the REE is probably the result of the

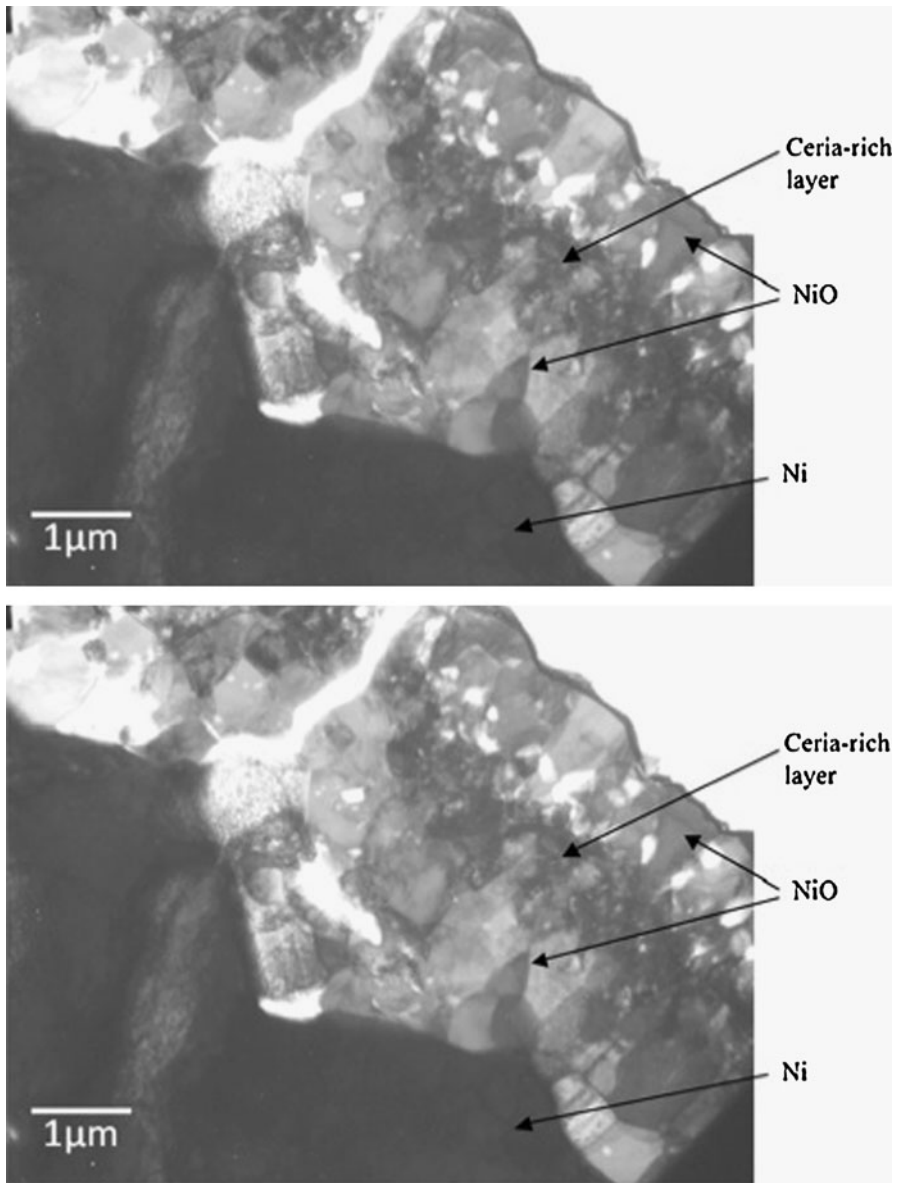


Fig. 10 Bright field TEM image of Ni which was oxidized for 15 min at 800 °C in air, coated with CeO₂ following pre-oxidation and then re-exposed for 50 h

dopant “decreasing the flux of outward diffusing Ni in some part of the oxide scale” but no single mechanism describes all the results.

There are, indeed, a number of mechanisms which could result in the reduced growth rate of NiO in the presence of a RE dopant.

Blocking Layer Formed by the Deposit

Numerous cross-sectional observations of the NiO formed on CeO₂ doped Ni (e.g. Fig. 1d) indicate that the CeO₂ does not form a continuous barrier layer. However, the observations by XTEM (e.g. Fig. 3) indicate that the layer may be continuous in some locations. Selected area diffraction from the layer indicated it remained as unreacted CeO₂, which is consistent with the Ni–Ce–O phase diagram [16]. An approximate calculation of the flux of oxygen through the CeO₂ layer was performed using a simple Fick's first law approach with the oxygen diffusivity assumed to be constant, and the oxygen transference number assumed to be unity.

$$J_{\text{O}} = D_{\text{O}} \frac{C''_{\text{V}_o} - C'_{\text{V}_o}}{x} \quad (1)$$

The CeO₂ at the oxide-gas interface was assumed to be in equilibrium with $p_{\text{O}_2} = 0.21$ atm, and the p_{O_2} at the CeO₂–Ni interface was assumed to be the Ni/NiO dissociation pressure. The oxygen vacancy gradient was calculated using these values, and the relevant data from Mogensen et al. [17]. This was combined with diffusivity data from Kamiya et al. [18] to calculate the flux of oxygen through a 200 nm thick layer of CeO₂. The flux was converted to a linear rate of mass change which is plotted in Fig. 11 along with the mass change for the diffusion controlled growth of NiO. The plot shows that if a 200 nm layer of CeO₂ was placed on NiO, the growth of the oxide would initially be controlled by oxygen diffusion through the ceria layer, but, after approximately 1 h, the flux of oxygen would be great enough to allow parabolic oxidation. This shows that the growth rate of NiO grown after short times would not be diminished by an external layer with the oxygen permeability of ceria.

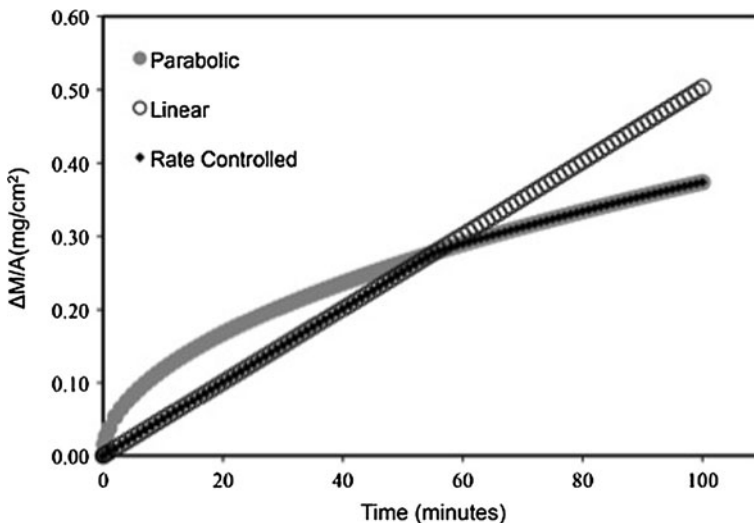
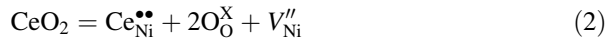


Fig. 11 Plot of specific mass change versus time for NiO growth controlled by diffusion in the growing oxide and by oxygen diffusion through a 200 nm thick layer of CeO₂ at 800 °C

Doping Effect

The incorporation of CeO₂ into NiO presumably occurs as



This equilibrium indicates the concentration of cation vacancies would tend to be increased by Ce-doping which would increase the outward flux of Ni ions rather than decrease it as is observed experimentally.

Poisoned Interface Model

The results from EDS analysis, both in SEM and XTEM, and SNMS analysis indicate that all of the Ce is segregated in the outer portions of the scale and was at or below the limit of detection at the Ni/NiO interface. These observations coupled with the results for the preoxidized Ni indicate that the PIM does not describe the REE of Ce on the growth of NiO.

Dopant Blocking Grain Boundary Diffusion of Ni Cations

Still another possible mechanism for the REE produced by CeO₂ in Ni is blocking of cationic transport along grain boundaries in the NiO scales. The XTEM observations in this study have shown Ce is segregated at NiO grain boundaries in the outer portions of the scale. Atkinson et al. [19] have reported that the oxidation of Ni is controlled by the outward diffusion of Ni ions along grain boundaries in the NiO film at temperatures below about 1,100 °C. The lattice diffusion coefficient for Ni ions is much larger than that for O ions, as would be expected from the defect structure of NiO [20]. However, the diffusion coefficients for Ni ions in low-angle and high-angle grain boundaries are larger still. The relative contributions to scale growth of bulk and grain boundary diffusion will depend on the temperature and the oxide grain size. It is generally observed that oxide scales growing on metals have rather fine grain sizes (on the order of a μm) so boundary diffusion can predominate to quite high temperatures. It is reported for NiO that boundary diffusion has a similar p_{O_2} -dependence to bulk diffusion [20] which suggests that similar point defects control both processes. The absence of a REE at 1,300 °C would be consistent with the bulk cation transport control of NiO growth at this temperature. Similarly, Haugsrud [21] observed that when CeO₂ doped Cu and Co were oxidized at temperatures at which lattice diffusion was rate controlling, 700 and 900 °C, respectively, the REE was absent.

It is known that many solute cations present in oxides will segregate to the oxide grain boundaries if there is substantial size mismatch with the host cation. Johnson has found that equilibrium segregation of solute based on a simple size misfit model adequately predicts the behavior of solutes in MgO, and Al₂O₃ [22], and many cations whose ionic radius differs by more than 10 % from that of Ni²⁺ have been found to segregate to the NiO grain boundaries [5, 23, 24].

There is evidence that the presence of misfitting ions in NiO grain boundaries suppresses diffusion. Experimentally, Atkinson et al. [20] found that the segregation

of Ca and Si in NiO bicrystals decreased nickel diffusion along boundaries and Duffy and Tasker [23] approached the effect of ceria in NiO grain boundaries using atomistic modeling, finding that the presence of an isolated Ce^{4+} ion in a grain boundary increases the activation energy for the diffusion of vacancies to a value greater than the activation energy of bulk diffusion.

The exact mechanism by which solutes inhibit diffusion along oxide grain boundaries is not presently agreed upon. If, indeed, cation vacancies control diffusion in both the grain boundaries and bulk NiO [20] the presence of Ce in the grain boundaries might be expected to increase the defect concentration according to Eq. 1. However, the difference in size and charge of solute ions may produce defect clusters in the boundary, limiting the mobility of vacancies or the introduction of misfitting ions into a grain boundary may change the vacancy migration path as a result of the physical distortion.

The combination of all the above results is entirely consistent with the REE of Ce on the oxidation of Ni at 800 °C being the result of blocking of grain boundary transport of cations within the NiO scale as proposed earlier for the REE effect in chromia [7, 8]. It should be remarked that another variant of this mechanism, the “dynamic segregation theory” [25] includes segregation at the metal/oxide interface as a precursor to segregation along the oxide grain boundaries. The absence of Ce at the Ni/NiO interface and the occurrence of the REE for preoxidized Ni indicate interface segregation is not necessary although it could indeed occur, particularly if the reactive element was contained within the alloy prior to oxidation.

Conclusions

The addition of CeO_2 to the surface of nickel altered the oxidation behavior of nickel in a manner consistent with the literature description of the REE. When nickel was pre-oxidized prior to ceria deposition, separating ceria from the metal/oxide interface, the ‘reactive element effect’ was still observed. Under these conditions the PIM cannot explain the decrease in the rate of oxidation. It is proposed that direct segregation of Ce^{4+} ions to the NiO grain boundaries decreases the cationic flux through the grain boundaries, decreasing the overall oxidation rate.

Acknowledgments Financial support of this study by the Office of Naval Research through Grant No. N00014-09-1-0564 is gratefully acknowledged.

References

1. R. W. Jackson, J. P. Leonard, F. S. Pettit and G. H. Meier, *Solid State Ionics* **179**, 2111 (2008).
2. R. W. Jackson, J. P. Leonard, L. Niewolek, W. J. Quadackers, F. S. Pettit and G. H. Meier, *Materials Science Forum* **595–598**, 1057 (2008).
3. A. A. Moosa, S. J. Rothman and L. J. Nowicki, *Oxidation of Metals* **24**, 115 (1985).
4. A. A. Moosa and S. J. Rothman, *Oxidation of Metals* **24**, 133 (1985).
5. R. Haugsrud, A. E. Gunnaes and O. Nilsen, *Oxidation of Metals* **3**, (4), 215 (2003).
6. R. Haugsrud, *Corrosion Science* **45**, 1289 (2003).
7. G. M. Ecer and G. H. Meier, *Oxidation of Metals* **13**, 159 (1979).

8. G. M. Ecer, R. B. Singh and G. H. Meier, *Oxidation Metals* **18**, 53 (1982).
9. P. Y. Hou and J. Stringer, *Materials Science and Engineering* **A202**, 1 (1995).
10. B. Pieraggi and R. A. Rapp, *Journal of Electrochemical Society* **140**, 2844 (1993).
11. B. Pieraggi, R. A. Rapp and J. P. Hirth, *Oxidation of Metals* **44**, 63 (1995).
12. A. Strawbridge and R. A. Rapp, *Journal of the Electrochemical Society* **141**, 1905 (1994).
13. J. P. Hirth and T. E. Mitchell, *Acta Materialia* **56**, 5701 (2008).
14. W. Bock, M. Kopnarsk and H. Oechsner, *Fresenius' Journal of Analytical Chemistry* **353**, 510 (1995).
15. W. J. Quadackers, A. Elschner, W. Speier and H. Nickel, *Applied Surface Science* **52**, 271 (1991).
16. N. Solak, M. Zinkevich, and F. Aldinger, *Fuel Cells* **6**, 87 (2006).
17. M. Mogensen, N. M. Sammes and G. A. Tompsett, *Solid State Ionics* **129**, 63 (2000).
18. M. Kamiya, E. Shimada, Y. Ikuma, M. Komatsu and H. Haneda, *Journal of the Electrochemical Society* **147**, 1222 (2000).
19. A. Atkinson, R. I. Taylor, and A. E. Hughes, *Philosophical Magazine*, **A45**, 823 (1982).
20. A. Atkinson, D. P. Moon, D. W. Smart and R. I. Taylor, *Journal of Materials Science* **21**, 1747 (1986).
21. R. Haugrud, *Corrosion Science* **44**, 1569 (2002).
22. W. C. Johnson, *Metallurgical Transaction A* **8A**, 1413 (1977).
23. D. M. Duffy and P. W. Tasker, *Philosophical Magazine* **A54**, 759 (1986).
24. R. Haugrud, A. E. Gunnaes and C. R. Simon, *Oxidation of Metals* **56**, 453 (2001).
25. B. A. Pint, *Oxidation of Metals* **45**, 1 (1996).